**Preprint**: This is a preprint of a contribution presented at the XLVIII International Summer School-Conference "Advanced Problems in Mechanics", June 21-26, 2020, St. Petersburg, Russia and submitted for peer review.

# Approximating unstable operation speeds of automatic ball balancers based on design parameters

Lars Spannan(✉)[0000-0003-3237-4405] and Elmar Woschke[0000-0002-8396-8265]

Otto von Guericke University, 39106 Magdeburg, Germany,
{lars.spannan, elmar.woschke}@ovgu.de

**Abstract.** Automatic balancers present a modular possibility to counteract variable rotor unbalances during operation. Two or more balancing masses, usually spheres, can orbit in a fluid-filled annular cavity whose axis of symmetry coincides with the rotor axis. At supercritical speeds the masses – driven by the rotor deflection – tend towards stationary positions inside the cavity opposing the primary rotor unbalance. Related to the phenomenon of rotating shafts being captured at resonances due to insufficient drive power, automatic ball balancers inhibit operation speed bands with non-synchronous vibrations where the rotor surpassed the resonance but the balls continue to orbit with the eigenfrequency with respect to the inertial system. As a result, the balancing masses do not take stationary positions inside the cavity and the rotor is excited not only by the primary unbalance but also by the sub-synchronously orbiting balancing masses. The width of the operation speed band exhibiting non-synchronous behaviour depends on the balancing masses, the orbit radius, external damping of the rotor and viscous damping of the balls due to the fluid inside the cavity. For a planar oscillator in isotropic supports with a balancer containing two balancing balls, an explicit correlation between the stability border and the fluid damping is presented. In order to parameterize the fluid damping model, the drag on spheres in annular cavities is examined and a proposed relation based on the cavity geometry and the fluid properties is presented.

**Keywords:** automatic balancing, stability, sub-synchronous vibration

## 1 Introduction

Rotating machinery can encounter variable mass distribution during operation, leading to unbalance excitation, which cannot be addressed by conventional balancing at the beginning of the product life cycle. Examples for aforementioned systems are washing machines, centrifuges for medical research and optical disc drives with varying content as well as grinding machines whose discs are worn unevenly.

To reduce variable unbalance excitations, automatic ball balancers (ABB) can be equipped to the rotor, counteracting the uneven mass distribution with

**Preprint**: This is a preprint of a contribution presented at the XLVIII International Summer School-Conference "Advanced Problems in Mechanics", June 21-26, 2020, St. Petersburg, Russia and submitted for peer review.

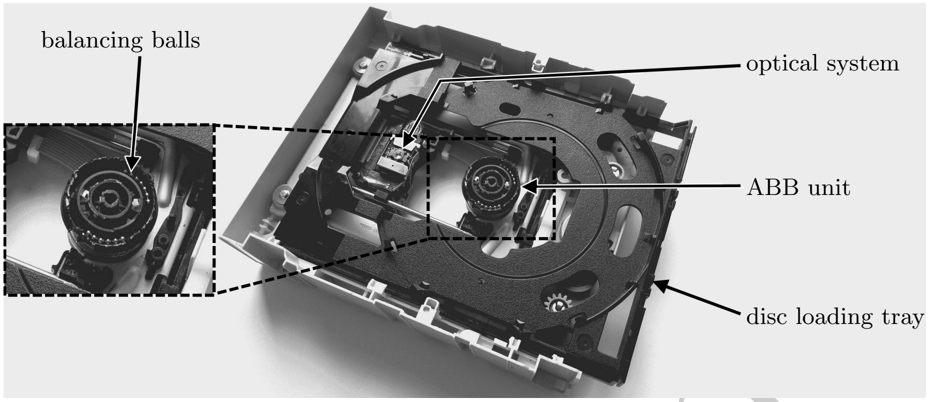


**Fig. 1.** Partially disassembled DVD Writer with ABB unit (pried open) to counterbalance variable disc unbalances.

freely movable masses (balls) inside an annular cavity whose symmetry axis coincides with the rotor axis, see Fig. 1 for an example application in an optical disc drive.

Driven by inertial effects resulting from the common deflection of the rotor and the ABB, the balancing balls move towards the orbital position with maximum distance to the axis of rotation. Resulting from this passive functional pricipal, ABBs only achieve the desired effect of balancing at super-critical operation, where the rotor displacement and the unbalance excitation have undergone the typical phase shift when passing through resonance.

In addition to the critical speed, which has to be surpassed for the intended operation of ABBs, a speed domain of unstable operation, which prevents the desired positioning of the balls just above the critical speed, has to be surpassed as well. The extent of this domain depends on the design parameters of the rotating system, in particular external damping and the selected fluid[1] with which the cavity is filled and is environing the balancing balls.

In the presented study, an explicit calculation of the unstable speed range for isotropically supported planar rotor systems with one ABB unit incorporating two balancing balls is derived. Section 2 describes the equations of motion of the planar system and Section 3 recapitulates the transformations used to gain a generalized eigenvalue problem whose frequency-dependent eigenvalues provide information about the stability of the operation, as presented in [1]. In Section 4 the Routh-Hurwitz criterion is applied to the eigenvalue problem and with the assumption of isotropic support of the rotor, an explicit relation between the viscous damping of the fluid, the external damping, the eigenfrequency of the rotor system and the balancing ball mass and orbit radius is deducted. Finally, a conclusion and outlook is given in Section 5.

[1] Air is used in the most rudimentary design, which has low viscous damping.

Preprint: This is a preprint of a contribution presented at the XLVIII International Summer School-Conference "Advanced Problems in Mechanics", June 21-26, 2020, St. Petersburg, Russia and submitted for peer review.

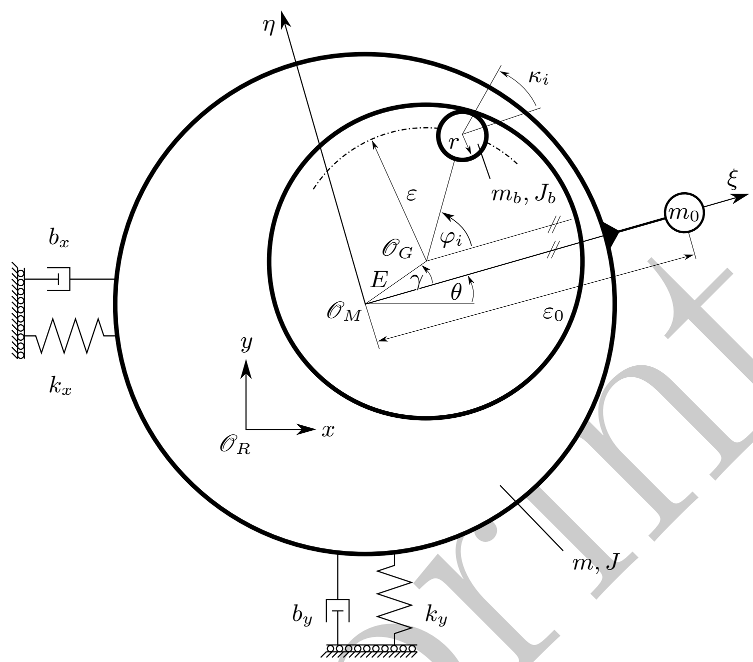


**Fig. 2.** Translational oscillator with primary unbalance and one counterbalancing mass of a balancer with eccentricity.

## 2 Equations of Motion

Let $m$ and $J$ be the mass and mass moment of inertia of a planar rotor in the $x$–$y$ plane, Fig. 2, excited by the primary unbalance mass $m_0$ located $\varepsilon_0$ away from the center of mass $\mathscr{O}_M$ of the balanced rotor. The rotor is mounted orthotropically described by linear stiffnesses $k_x$ and $k_y$ and viscous damping coefficients $b_x$ and $b_y$, respectively. The rotation angle $\theta$ of the rotor is indicated by the position of the primary unbalance and describes the orientation of the rotor fixed coordinate system $\xi$–$\eta$.

Due to manufacturing and assembly tolerances, the raceway of the balancing balls may encounter an eccentric geometric center $\mathscr{O}_G$, described by angle $\gamma$ and eccentricity $E$. The balancing balls of mass $m_b$ and radius $r$ can move inside the cavity on an orbit with radius $\varepsilon$. The rotor-fixed orbital position of ball $i$ with respect to the primary unbalance is described by $\varphi_i$.

Considering an ABB with two identical balls sharing the same orbit, the potential and kinetic energy

$$U = \frac{1}{2}\left(k_x x^2 + k_y y^2\right) \tag{1}$$

$$T = \frac{1}{2}\Big(m\left(\dot{x}^2 + \dot{y}^2\right) + J\dot{\theta}^2 + m_0\left(\dot{x}_0^2 + \dot{y}_0^2\right)\Big) + \sum_{i=1}^{2}\frac{m_b\left(\dot{x}_i^2 + \dot{y}_i^2\right) + J_b\dot{\kappa}_i^2}{2} \tag{2}$$

can be formulated. Inserting the no-slip rolling condition, the coordinates of the centres of mass can be expressed in terms of $x$, $y$, $\theta$ and $\varphi_i$

$$\begin{aligned} x_0 &= x + \varepsilon_0 \cos(\theta), \quad x_i = x + \varepsilon \cos(\theta + \varphi_i) + E \cos(\theta + \gamma), \\ y_0 &= y + \varepsilon_0 \sin(\theta), \quad y_i = y + \varepsilon \sin(\theta + \varphi_i) + E \sin(\theta + \gamma), \\ \kappa_i &= \theta - \frac{\varepsilon}{r} \varphi_i. \end{aligned}$$

In accordance with [2,3,4] and others, the viscous effect on the balls due to the fluid are modelled in a linear manner by the torque

$$M_D = -\beta \dot{\varphi}_i. \tag{3}$$

In combination with the translatoric damping forces and an external damping torque

$$F_{bx} = -b_x \dot{x}, \qquad F_{by} = -b_y \dot{y}, \qquad M_{\beta_0} = -\beta_0 \dot{\theta},$$

evaluation of the Euler–Lagrange equations yields, with $M = m + m_0 + \sum_{i=1}^{2} m_i$, a system of five differential equations

$$\begin{aligned} &M\ddot{x} + b_x \dot{x} + k_x x = \\ &\quad \left( m_0 \varepsilon_0 \sin(\theta) + \sum_{i=1}^{2} E m_b \sin(\gamma + \theta) + m_b \varepsilon \sin(\theta + \varphi_i) \right) \ddot{\theta} \\ &\quad + \left( m_0 \varepsilon_0 \cos(\theta) \dot{\theta} + \sum_{i=1}^{2} E m_b \cos(\gamma + \theta) \dot{\theta} + m_b \varepsilon \left( \dot{\theta} + \dot{\varphi}_i \right) \cos(\theta + \varphi_i) \right) \dot{\theta} \\ &\quad + \sum_{i=1}^{2} m_b \varepsilon \left( \dot{\theta} + \dot{\varphi}_i \right) \cos(\theta + \varphi_i) \dot{\varphi}_i + m_b \varepsilon \sin(\theta + \varphi_i) \ddot{\varphi}_i \end{aligned} \tag{4}$$

$$\begin{aligned} &M\ddot{y} + b_y \dot{y} + k_y y = \\ &\quad - \left( m_0 \varepsilon_0 \cos(\theta) + \sum_{i=1}^{2} E m_b \cos(\gamma + \theta) + m_b \varepsilon \cos(\theta + \varphi_i) \right) \ddot{\theta} \\ &\quad + \left( m_0 \varepsilon_0 \sin(\theta) \dot{\theta} + \sum_{i=1}^{2} E m_b \sin(\gamma + \theta) \dot{\theta} + m_b \varepsilon \left( \dot{\theta} + \dot{\varphi}_i \right) \sin(\theta + \varphi_i) \right) \dot{\theta} \\ &\quad + \sum_{i=1}^{2} m_b \varepsilon \left( \dot{\theta} + \dot{\varphi}_i \right) \sin(\theta + \varphi_i) \dot{\varphi}_i - m_b \varepsilon \cos(\theta + \varphi_i) \ddot{\varphi}_i \end{aligned} \tag{5}$$

$$\begin{aligned}
&\left(J + m_0\varepsilon_0^2 + \sum_{i=1}^{2} J_b + m_b E^2 + m_b\varepsilon^2 + 2Em_b\varepsilon\cos(\gamma-\varphi_i)\right)\ddot{\theta} \\
&+ \left(\beta_0 + \sum_{i=1}^{2} 2Em_b\varepsilon\sin(\gamma-\varphi_i)\dot{\varphi}_i\right)\dot{\theta} = M_0 \\
&+ \left(m_0\varepsilon_0\sin(\theta) + \sum_{i=1}^{2} m_b E\sin(\gamma+\theta) + m_b\varepsilon\sin(\theta+\varphi_i)\right)\ddot{x} \\
&- \left(m_0\varepsilon_0\cos(\theta) + \sum_{i=1}^{2} Em_b\cos(\gamma+\theta) + m_b\varepsilon\cos(\theta+\varphi_i)\right)\ddot{y} \\
&- \sum_{i=1}^{2}\left(Em_b\varepsilon\cos(\gamma-\varphi_i) - \frac{J_b\varepsilon}{r} + m_b\varepsilon^2\right)\ddot{\varphi}_i + Em_b\varepsilon\sin(\gamma-\varphi_i)\dot{\varphi}_i^2 \qquad (6)
\end{aligned}$$

$$\begin{aligned}
&\left(\frac{J_b\varepsilon^2}{r^2} + m_b\varepsilon^2\right)\ddot{\varphi}_i + \beta\dot{\varphi}_i = \left(\frac{J_b\varepsilon}{r} - Em_b\varepsilon\cos(\gamma-\varphi_i) - m_b\varepsilon^2\right)\ddot{\theta} \\
&+ m_b\varepsilon\left(E\sin(\gamma-\varphi_i)\dot{\theta}^2 + \sin(\theta+\varphi_i)\ddot{x} - \cos(\theta+\varphi_i)\ddot{y}\right) \quad \forall i \in \{1,2\}. \qquad (7)
\end{aligned}$$

### 2.1 Identification of the viscous drag coefficient

Assuming a quasi steady state with the fluid flow velocity $v_{\text{flow}}$ equal to the speed of the rotor and small orbit velocities $\dot{\varphi}_i$ of the balls with respect to the rotor, a Stokes flow regime can be assumed, leading to a reciprocal relation between the Reynolds number

$$\mathrm{Re} = \frac{2v_{\text{flow}}r}{\nu_{\text{fluid}}} \approx \frac{2\dot{\varphi}_i\varepsilon r}{\nu_{\text{fluid}}}, \qquad (8)$$

with $\nu_{\text{fluid}}$ being the kinematic viscosity of the fluid, and the resulting drag coefficient $c_d$. Therefore the product $c_d\,\mathrm{Re}$ can be represented by a scalar, which depends on the geometry of the annular cavity and the relative ball size. Inserting the drag force

$$F_D = \frac{1}{2}\rho_{\text{fluid}}\pi r^2 c_d v_{\text{flow}}^2\,\mathrm{sign}(v_{\text{flow}}), \qquad (9)$$

with $\rho_{\text{fluid}}$ being the fluid density, into Eq. (3) leads to

$$\beta = c_d\,\mathrm{Re}\,\frac{\pi}{4}\rho_{\text{fluid}}\nu_{\text{fluid}} r\varepsilon^2. \qquad (10)$$

An appropriate value for $c_d\,\mathrm{Re}$ can be determined empirically, see [5,6], or by CFD analysis for the specific geometry of the annular cavity and the balancing balls. One suitable estimation results from the widely studied drag forces on a sphere in contact with a flat wall, e.g. $c_d\,\mathrm{Re} = 322$, which was identified empirically in [7].

**Preprint**: This is a preprint of a contribution presented at the XLVIII International Summer School-Conference "Advanced Problems in Mechanics", June 21-26, 2020, St. Petersburg, Russia and submitted for peer review.

## 3 Condition for stable balancing

Following the procedure presented in [1], Equations (4), (5) and (7), evaluated for $i = \{1, 2\}$, can be transformed utilizing the Krylov-Bogoliubov-Mitropolsky method [8]. The coordinates $x$ and $y$ are substituted by

$$\begin{aligned} x = \tilde{x} &= A_x \cos(\theta) - B_x \sin(\theta), & y = \tilde{y} &= A_y \sin(\theta) + B_y \cos(\theta), \\ \dot{\tilde{x}} &= -\dot{\theta} A_x \sin(\theta) - \dot{\theta} B_x \cos(\theta), & \dot{\tilde{y}} &= \dot{\theta} A_y \cos(\theta) - \dot{\theta} B_y \sin(\theta), \\ \ddot{\tilde{x}} &= \partial \dot{\tilde{x}} / \partial t, & \ddot{\tilde{y}} &= \partial \dot{\tilde{y}} / \partial t, \end{aligned} \tag{11}$$

yielding the additional conditions

$$\dot{A}_x = \dot{B}_x \sin(\dot{\theta} t) / \cos(\dot{\theta} t), \qquad \dot{B}_y = -\dot{A}_y \sin(\dot{\theta} t) / \cos(\dot{\theta} t). \tag{12}$$

Considering the steady state, e.g. $\dot{\theta} = \omega$, $\ddot{\theta} = 0$, $\ddot{\varphi}_1 = 0$ and $\ddot{\varphi}_2 = 0$, a system of six ordinary differential equations (ODEs) is formed in terms of $A_x$, $B_x$, $A_y$, $B_y$, $\varphi_1$ and $\varphi_2$. Approximation of the ODEs by their integral mean over one revolution removes the trigonometric terms in $\omega t$.

Following a linear perturbation analysis, i.e. substituting

$$\begin{aligned} A_x &= A_{0x} + \Delta A_x, & B_x &= B_{0x} + \Delta B_x, & A_y &= A_{0y} + \Delta A_y, \\ B_y &= B_{0y} + \Delta B_x, & \varphi_1 &= \varphi_{01} + \Delta \varphi_1, & \varphi_2 &= \varphi_{02} + \Delta \varphi_2, \end{aligned}$$

expanding the trigonometric terms in $\Delta\varphi_1$ and $\Delta\varphi_2$ and neglecting terms of higher order, the system of linear ODEs of first order $\underline{\underline{A}}\,\dot{\underline{z}} + \underline{\underline{B}}\,\underline{z} = \underline{0}$ with $\underline{z} = [\Delta A_x, \Delta B_x, \Delta A_y, \Delta B_y, \Delta\varphi_1, \Delta\varphi_2]^T$,

$$\underline{\underline{A}} = \begin{bmatrix} -1 & 0 & 0 & 0 & \frac{m_b \varepsilon \sin(\varphi_{01})}{M} & \frac{m_b \varepsilon \sin(\varphi_{02})}{M} \\ 0 & -1 & 0 & 0 & -\frac{m_b \varepsilon \cos(\varphi_{01})}{M} & -\frac{m_b \varepsilon \cos(\varphi_{02})}{M} \\ 0 & 0 & -1 & 0 & \frac{m_b \varepsilon \sin(\varphi_{01})}{M} & \frac{m_b \varepsilon \sin(\varphi_{02})}{M} \\ 0 & 0 & 0 & -1 & -\frac{m_b \varepsilon \cos(\varphi_{01})}{M} & -\frac{m_b \varepsilon \cos(\varphi_{02})}{M} \\ \frac{\omega \cos(\varphi_{01})}{2} & \frac{\omega \sin(\varphi_{01})}{2} & \frac{\omega \cos(\varphi_{01})}{2} & \frac{\omega \sin(\varphi_{01})}{2} & \frac{\beta}{m_b \varepsilon} & 0 \\ \frac{\omega \cos(\varphi_{02})}{2} & \frac{\omega \sin(\varphi_{02})}{2} & \frac{\omega \cos(\varphi_{02})}{2} & \frac{\omega \sin(\varphi_{02})}{2} & 0 & \frac{\beta}{m_b \varepsilon} \end{bmatrix},$$

and

$$\underline{\underline{B}} = \begin{bmatrix} -\frac{b_x}{2M} & \frac{\omega}{2} - \frac{k_x}{2M\omega} & 0 & 0 & \frac{m_b \omega \varepsilon \cos(\varphi_{01})}{2M} & \frac{m_b \omega \varepsilon \cos(\varphi_{02})}{2M} \\ -\frac{\omega}{2} + \frac{k_x}{2M\omega} & -\frac{b_x}{2M} & 0 & 0 & \frac{m_b \omega \varepsilon \sin(\varphi_{01})}{2M} & \frac{m_b \omega \varepsilon \sin(\varphi_{02})}{2M} \\ 0 & 0 & -\frac{b_y}{2M} & \frac{\omega}{2} - \frac{k_y}{2M\omega} & \frac{m_b \omega \varepsilon \cos(\varphi_{01})}{2M} & \frac{m_b \omega \varepsilon \cos(\varphi_{02})}{2M} \\ 0 & 0 & -\frac{\omega}{2} + \frac{k_y}{2M\omega} & -\frac{b_y}{2M} & \frac{m_b \omega \varepsilon \sin(\varphi_{01})}{2M} & \frac{m_b \omega \varepsilon \sin(\varphi_{02})}{2M} \\ \frac{\omega^2 \sin(\varphi_{01})}{2} & -\frac{\omega^2 \cos(\varphi_{01})}{2} & \frac{\omega^2 \sin(\varphi_{01})}{2} & -\frac{\omega^2 \cos(\varphi_{01})}{2} & 0 & 0 \\ \frac{\omega^2 \sin(\varphi_{02})}{2} & -\frac{\omega^2 \cos(\varphi_{02})}{2} & \frac{\omega^2 \sin(\varphi_{02})}{2} & -\frac{\omega^2 \cos(\varphi_{02})}{2} & 0 & 0 \end{bmatrix}$$

is obtained.

By solving the eigenvalue problem of the system

$$\left(\underline{\underline{B}} + \lambda\,\underline{\underline{A}}\right) \underline{v} = \underline{0} \tag{13}$$

of order six and determining if all eigenvalues $\lambda$ have negative real parts

$$\Re(\lambda) < 0 \quad \forall \lambda \,, \tag{14}$$

the stability of the system can be obtained for a given angular frequency $\omega$ of the rotor. However, numerical methods show inaccuracies when $\varphi_{01} = -\varphi_{02} = \pi/2$ or $\varphi_{01} = -\varphi_{02} = \pi$, i.e. when the ABB eccentricity is zero and the primary unbalance is very low or very high, respectively. This follows from the resulting poor condition of the matrices. Alternatively, the sixth order characteristic polynomial of Eq. (13) can be tested with the Routh–Hurwitz stability criterion [9]. With the variation of one design parameter of the ABB, a stability chart can be obtained, depicting the stable operating speeds, see Fig. 3. Since the choice of fluid is barely subject to boundary conditions, the variation of the fluid properties is well suited to influence the behaviour of the ABB unit. Hence, the stability maps are presented in the $\beta$–$\omega$ space.

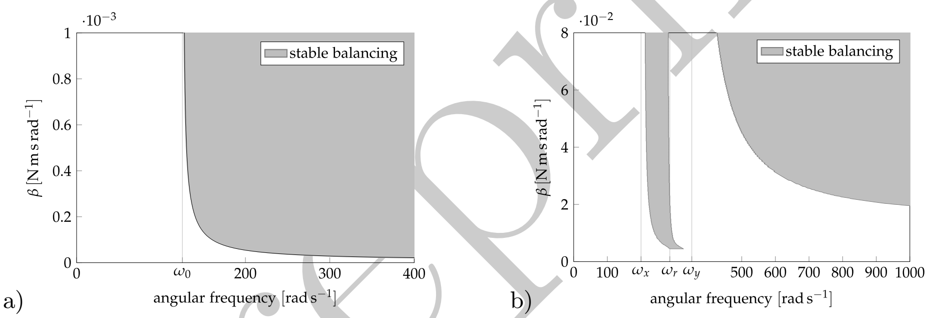


**Fig. 3.** Stability chart examples for variable viscous parameter $\beta$ for the case of (a) isotropic and (b) orthotropic ($k_x < k_y$) supports.

As can be seen from the graphs, stable balancing can only be achieved above the natural frequency if the viscous parameter of the liquid is sufficiently high. In the case of orthotropic supports, the stability area is divided in two regions, as only forward whirling motions of the rotor can be balanced [10].

## 4 Explicit stability border for the isotropic eccentricity free case

For a given rotor and ABB configuration with two balls, the stability chart can be readily obtained as presented above. Assuming isotropic supports, i.e. $k_x = k_y = k$, $b_x = b_y = b$ and therefore $k/M \equiv \omega_0^2$, and no eccentricity of the orbit raceway, the balancing balls will be positioned symmetrically in order to counterbalance the primary unbalance, resulting in

$$\varphi_{02} = -\varphi_{01}, \quad \pi/2 \leq \varphi_{01} \leq \pi \,. \tag{15}$$

Simplifying the matrices in Eq. (13) under the assumptions stated above, the characteristic equation can be written in a factorised form

$$
\begin{aligned}
0 =& 16M^4(m_b\varepsilon)^2\omega^4\left[M^2\left(\omega^2-\omega_0^2\right)^2+\omega^2\left(2M\lambda+b\right)^2\right] \\
&\Big[4(m_b\varepsilon)^4\left(\lambda^2\omega^6+\left(2\lambda^2\omega^2+\omega^4\right)^2\right)\sin^2\left(\varphi_{01}\right)\cos^2\left(\varphi_{01}\right) \\
&+\beta\lambda\Big(2(m_b\varepsilon)^2\omega^4\left(M\left(\omega^2-\omega_0^2\right)+3\lambda b\right)+M^2\beta\lambda\left(\omega^2-\omega_0^2\right)^2 \\
&+4M\lambda^2\omega^2\left((m_b\varepsilon)^2\left(2\omega^2+\omega_0^2\right)+\beta\left(M\lambda+b\right)\right)+\beta\lambda\omega^2b^2\Big)\Big]. \qquad (16)
\end{aligned}
$$

From the first term in brackets follow the roots

$$
\lambda=-\frac{b}{2M}+i\frac{\omega_0^2-\omega^2}{2\omega} \quad \vee \quad \lambda=-\frac{b}{2M}+i\frac{\omega_0^2+\omega^2}{2\omega} \qquad (17)
$$

with negative real parts. The second term in brackets is a fourth order polynomial $a_4\lambda^4+a_3\lambda^3+a_2\lambda^2+a_1\lambda+a_0$ with the coefficients being rewritable as

$$
\begin{aligned}
a_0 =& 4\omega^2\left(4(m_b\varepsilon)^4\omega^2\sin^2\left(\varphi_{01}\right)\cos^2\left(\varphi_{01}\right)+M^2\beta^2\right), \\
a_1 =& 4M\beta\omega^2\left(2(m_b\varepsilon)^2\omega^2+(m_b\varepsilon)^2\omega_0^2+\beta b\right), \\
a_2 =& M^2\beta^2\left(\omega^2-\omega_0^2\right)^2+ \\
&\omega^2\left(20(m_b\varepsilon)^4\omega^4\sin^2\left(\varphi_{01}\right)\cos^2\left(\varphi_{01}\right)+6(m_b\varepsilon)^2\beta\omega^2 b+\beta^2b^2\right), \qquad (18) \\
a_3 =& 2(m_b\varepsilon)^2M\beta\omega^4\left(\omega-\omega_0\right)\left(\omega+\omega_0\right), \\
a_4 =& 4(m_b\varepsilon)^4\omega^8\sin^2\left(\varphi_{01}\right)\cos^2\left(\varphi_{01}\right).
\end{aligned}
$$

Since $a_4>0$, it is necessary and sufficient [9] that $a_0>0$, $a_1>0$, $a_2>0$, $a_3>0$ and

$$
0<a_3(a_1a_2-a_0a_3)-a_4a_1^2. \qquad (19)
$$

From $a_3>0$ follows the familiar condition $\omega>\omega_0$ for automatic balancing at super critical speeds. Differentiation of the right hand side of Eq. (19) with respect to $\varphi_{01}$ yields

$$
\frac{\mathrm{d}}{\mathrm{d}\varphi_{01}}a_3(a_1a_2-a_0a_3)-a_4a_1^2=-p\sin(4\varphi_{01}) \qquad (20)
$$

$$
\frac{\mathrm{d}^2}{\mathrm{d}\varphi_{01}^2}a_3(a_1a_2-a_0a_3)-a_4a_1^2=-4p\cos(4\varphi_{01}) \qquad (21)
$$

with

$$
\begin{aligned}
0<p=16(m_b\varepsilon)^4M^2\beta^2\omega^{12}\big(&\beta b\left(2\beta b+3(m_b\varepsilon)^2\omega^2\right)+ \\
&9(m_b\varepsilon)^2\omega_0^2\left(\beta b+(m_b\varepsilon)^2(\omega^2+\omega_0^2)\right)\big).
\end{aligned}
$$

The roots of Eq. (20) deliver possible extrema of the stability criterion at $\varphi_{01}=j\pi/4$, $j\in\{2,3,4\}$, depicted in Fig. 4. Evaluation of Eq. (21) shows that $\varphi_{01}=$

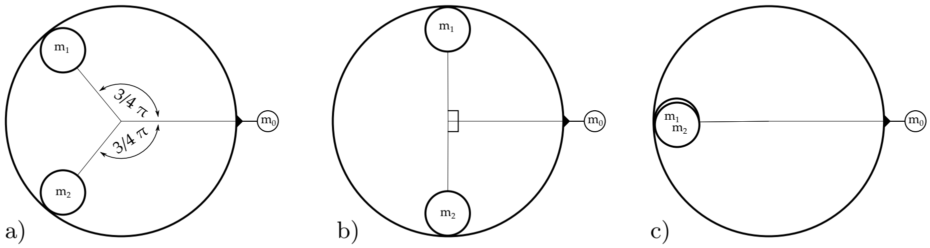


**Fig. 4.** Balancing ball positions resulting in extrema of the stability criterion. Primary unbalance magnitude: (a) Medium (b) low (c) high.

$3\pi/4$ is a minimum of the criterion, therefore the stability of the system is guaranteed if Eq. (19) holds for $\varphi_{01} = 3\pi/4$, which reads after factorization

$$\begin{aligned} 0 <& 8(m_b\varepsilon)^2 M^2 \beta^2 \omega^6 \left[\beta b(\omega^2 - \omega_0^2) - \omega_0^2 (m_b\varepsilon)^2 (\omega^2 + \omega_0^2)\right] \\ &\left[M^2\beta^2 \left(\omega^2 - \omega_0^2\right)^2 + \left(3(m_b\varepsilon)^2\omega^3 + \beta\omega b\right)^2\right]. \end{aligned}$$

Since the second braced term is always greater than zero, the criterion requires the first braced term to be positive and thus

$$\beta > \frac{(m_b\varepsilon)^2\omega_0^2}{b} \frac{\omega^2 + \omega_0^2}{\omega^2 - \omega_0^2}. \tag{22}$$

From Eq. (22) the limit

$$\beta_{\min} = \lim_{\omega\to\infty} \beta = \frac{(m_b\varepsilon)^2\omega_0^2}{b} \tag{23}$$

can be derived, describing a minimum required value for the viscous drag parameter $\beta$, in order to be able to pass the unstable operation of the ABB, see Fig. 5. With Eq. (10) these requirements can be expressed as a minimum dynamic fluid viscosity.

The assumptions of absence of raceway eccentricity and specific orbit positions of the counterbalancing masses are justified by the fact that these values are not subject to design, but are caused by manufacturing inaccuracies and the variable magnitude of the primary unbalance inherent to the application. Furthermore, sensitivity analyses of the stability considerations using Eq. (13) show only marginal influences on the stability border.

## 5 Conclusion and outlook

The problem of sub synchronous behaviour may be a minor issue in the design of ABB units. Since rotating machinery, which run above the first critical frequency, are operated with sufficient clearance to avoid substantial unbalance excitation.

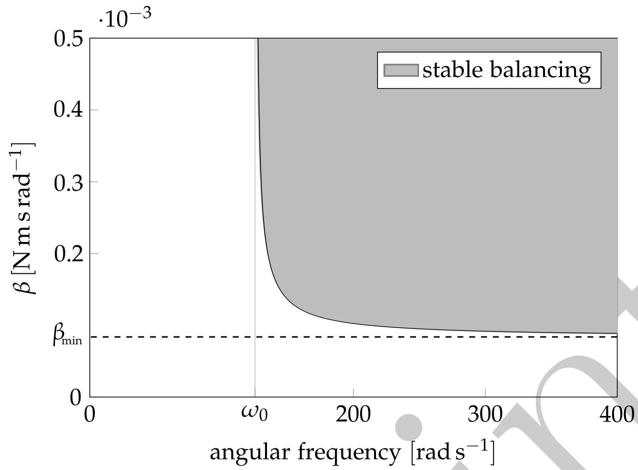


**Fig. 5.** Stability chart for an ABB in isotropic supports showing the minimum viscous parameter value required to surpass unstable operation

The frequency band of unstable behaviour, as shown in the stability maps, is often avoided due to already existing constraints concerning the operation speed. Nevertheless, the presented explicit determination of the stability border for ABB units in isotropic supports can simplify the estimation of stability problems significantly.

An interesting result emerges from the minimum fluid viscosity required to surpass the sub synchronous behaviour at all. This is most relevant, when air filled ABB units are utilized in order to avoid the design of sealing and filling procedures. Due to the low viscosity, ABB designs with air filled cavities are most prone to unstable behaviour if external damping is insufficient.

However, the presented model neglects the dissipative rolling friction between the balls and the raceway. This damping behavior leads to stabilization and thus smaller areas of instability. In addition, no suitable factorization of the characteristic equation of the orthotropically supported ABB system was found, which would allow an analogous evaluation of the criterion to derive explicit representations for the stability limits.

## References


1. Bykov VG, Kovachev AS (2018) Autobalancing of a rigid rotor in viscoelastic orthotropic supports considering eccentricity of the automatic ball balancer. AIP Conference Proceedings 1959(1):080,011, doi:10/gf3s79
2. Sharp R (1975) An analysis of a self-balancing system for rigid rotors. Journal of Mechanical Engineering Science 17(4):186–189, doi:10/bzcp8d
3. Lee J, Van Moorhem W (1996) Analytical and Experimental Analysis of a Self-Compensating Dynamic Balancer in a Rotating Mechanism. Journal of Dynamic Systems, Measurement, and Control 118(3):468–475, doi:10/fg8sdj

4. Sperling L, Merten F, Duckstein H (2000) Self-synchronization and Automatic Balancing in Rotor Dynamics. International Journal of Rotating Machinery 6(4):275–285, doi:10/d25fj2
5. Spannan L, Daniel C, Woschke E (2017) Experimental study on the velocity dependent drag coefficient and friction in an automatic ball balancer. Technische Mechanik 37(1):62–68, doi:10/gf3s8h
6. Spannan L, Daniel C, Woschke E (2018) Simulation of the ball kinetic in ball-type automatic balancing devices by solving the axisymmetric navier-stokes equations in annular cavities. In: Cavalca K, Weber H (eds) Proceedings of the 10th International Conference on Rotor Dynamics - IFToMM, vol 63, Springer, Cham, pp 109–118, doi:10/gf3s8f
7. Jan CD, Chen JC (1997) Movements of a sphere rolling down an inclined plane. Journal of Hydraulic Research 35(5):689–706, doi:10/bp4x9v
8. Kryloff N, Bogoliubov N (1947) Introduction to non-linear mechanics. Annals of Mathematics Studies, Princeton University Press, english translation
9. Popov EP (1962) The Dynamics of Automatic Control Systems. Pergamon Press
10. Ryzhik B, Sperling L, Duckstein H (2004) Auto-balancing of anisotropically supported rigid rotors. Technische Mechanik 24(1):37–50